Longitudinal Protection of Line Direction Based on VMD-HT and SVM

Guo Zhenwei, Li Haojie, Zhao Ruiqiang, Jiang Yongyan, Deng Yingcai

Abstract*—Transient direction longitudinal protection has the performance of ultra-high-speed operation, but it is difficult to identify the wave head under weak fault conditions. The sensitivity is not enough, and the reliability is low. To solve these problems, this paper proposes a novel fault current traveling wave differential direction relay which does not need to identify the traveling wave head. A longitudinal protection method based on multi-dimensional fault characteristics and working condition attributes is proposed to judge the fault direction. Firstly, a new fault direction characteristic is constructed by using the instantaneous amplitude difference of two lines. Two fault condition attributes, transient resistance, and start fault phase angle, are assigned to the fault direction feature, and the fault direction feature is sublimated from two-dimensional space to four-dimensional space with multiple information. Fault direction feature and fault condition attribute is used as SVM input. SVM was trained to judge fault direction with test samples. The trained SVM is used to judge the fault direction. Attributes of fault condition is coalesced into fault direction characteristics by SVM, so that fault direction traits contains fault condition attribute information. It overcame the impact of attributes of fault condition on transient protection, solved the problem of insufficient sensitivity of 10% fault protection, and improved protection reliability. In the end, EMTP-RV is used to verify the proposed algorithm's accuracy to judge the faults zone through lots number of simulations.

***Index Terms*—Transient direction longitudinal protection, Instantaneous amplitude difference, Fault condition attribute, VMD-HT, SVM**

I. Introduction

ACCURATE and rapid fault clearance is essential to enhance the transient reliability of the power system and increase the transmission capability of transmission lines [1]. Line protection based on power frequency is affected by power system oscillation, overload, and short-circuit point transient resistance. With the continuous improvement of power-grid's voltage level, the requirements for protection performance are increasingly stringent, bringing new challenges to the power system [2]-[4]. Conventional protection techniques relying on power frequency struggle to meet the demands of modern power grid development. [5]. In the actual power system, transmission-lines' distribution parameters have obvious characteristics, and the transient components generated when faults occur carry a wealth of fault information, e.g. fault time, fault type, and fault direction [6]. Protection based on fault transient components can swiftly recognize high-frequency components, realize ultra-high-speed safeguarding, and be unaffected by industrial-frequency oscillations and CT saturation [7]. Therefore, protection based on transient quantities has always been one of the key areas of research [8].

Longitudinal protection is widely used in ultra-high-voltage transmission lines because of its rapid response capability across the entire line [9]. Longitudinal protection mainly includes directional longitudinal protection and differential longitudinal protection. Reference [10] proposed a traveling wave differential longitudinal protection method by contrasting the calculated values of voltage traveling waves and current traveling waves at the far end with the measured values of current traveling waves at the home end. However, differential longitudinal protection calls for rigorous information coordination at both ends of the protection line, which is highly reliant on communication systems [11]. The directional longitudinal protection, on the other hand, has a low demand for communication and can cover the whole line by transmitting only the directional information, thus attracting much attention.

The key of directional longitudinal protection is fault direction judgment. A variety of modern signal processing techniques are widely used in transmission line transient travelling-wave directional protection to improve the performance of fault direction identification by fault transient information. These techniques include wavelet transform, variational mode decomposition (VMD), neural network methods, mathematical morphology, and Hilbert-Huang transform [12], [13]. VMD is a non-stationary signal decomposition algorithm, which can get rid of modal mixing in the course of iterative filtering , and has been applied in many fields such as fault location and fault detection in power systems [14], [15]. The energy of the forward and backward wave components is compared to establish the fault's orientation [16]. Reference [17] uses wavelet singular value to determine the reach time and singularity symbol of the fault travelling-wave head. The fault direction is determined by the ratio of the first voltage travelling-wave to

Manuscript received October 5, 2024; revised February 21, 2025.

This work was supported in part by the National Natural Science Foundation of China (52067005) and Guangxi Natural Science Foundation of China (2021GXNSFAA220061).

Guo Zhenwei is an associate professor of School of Mechanical and Electrical Engineering, Guilin University of Electronic Technology, Guilin Guangxi 541004, China. (e-mail: gzwcbf@sina.com).

Li Haojie is a postgraduate student of School of Mechanical and Electrical Engineering, Guilin University of Electronic Technology, Guilin Guangxi 541004, China. (corresponding author to provide phone:+86-13191194114; e-mail: lihj327@163.com).

Zhao Ruiqiang is a postgraduate student of School of Mechanical and Electrical Engineering, Guilin University of Electronic Technology, Guilin Guangxi 541004, China. (e-mail: 3295657367@qq.com).

Jiang Yongyan is a postgraduate student of School of Mechanical and Electrical Engineering, Guilin University of Electronic Technology, Guilin Guangxi 541004, China. (e-mail: 1583196429@qq.com).

Deng Yingcai is a postgraduate student of School of Mechanical and Electrical Engineering, Guilin University of Electronic Technology, Guilin Guangxi 541004, China. (e-mail: 2409389368@qq.com).

the current travelling-wave in the multi-frequency band [18], [19]. However, the reliability of these protection methods is impacted by the transient resistance or the first fault angle. When the transient resistance is high or first fault angle is small, the fault transient signal is significantly weakened, there is no clear fault characteristic, and protection performance is severely compromised, which may not meet the requirements. The reliability of traditional travelling-wave protection has been questioned for it relies on detecting the travelling wavehead [20]. In [21], it is pointed out that a smaller initial fault angle results in lower sensitivity of the transient travelling-wave directional protection. Moreover, within the ±18° range around the zero-crossing point of the initial fault angle, the reliability does not meet the required standards.

Reference [22] reduced the fault characteristics to a standard fault state to overcome the impacted of the start fault angle and transient resistance. However, the reduction effect of this method is not ideal, and the traditional fixed value setting method is still used. If different protection action values can be set based on varying fault conditions, the reliability of protection can be significantly improved [23], [24]. Therefore, if the fault characteristics can be correlated with the attributes of fault condition of transient resistance and start fault angle, the fault characteristic value can be investigated from the fault condition attribute and different action values can be set in accordance with different fault conditions during the fault judgment process, which will significantly enhance accuracy of fault judgment and the reliability of protection. The Support Vector Machine's (SVM) machine learning capabilities can be used to do this. As a supervised learning technique intended for both categorization and regression problems, SVM was initially introduced by Vapnik *et al.* in 1995. SVM has significant advantages in solving applied problems such as small samples, high dimensions and nonlinearity, and has been widely used in many fields such as state assessment, fault diagnosis, and pattern recognition [25]-[28].

In this paper, a novel transient direction relay on the basis of instantaneous amplitude difference of fault current traveling wave is proposed, and two-dimensional fault condition attributes, transient resistance and initial fault angle, are associated with the fault direction feature. The fault direction feature and the attributes of fault condition are combined to form composite fault features, and SVM is employed to assess the fault direction to mitigate the impact of fault condition attributes. The remaining articles are arranged as follows. Section 2 briefly describes the instantaneous amplitude method of the fault electrical wave. Section 3 describes the basic principle and processing of the proposal algorithm. In Section 4, lots of simulations verify the correctness of the algorithm. Section 5 describes the characteristics and benefits of the proposed algorithm.

II. Calculation of Instantaneous Amplitude of Fault Current Travelling Wave

A. Fault Signal VMD Decomposition

In this study, the fault signal is decomposed by VMD, enabling the extraction of its high-frequency components.

VMD decomposition overcomes the boundary effect and mode component aliasing problems in empirical mode decomposition (EMD) [29]. This approach reduces the non-stationary characteristics of complex, highly non-linear time series and yields more stable subcomponents spanning multiple frequency ranges. The VMD algorithm is more stable and accurate in the signal decomposition process, and less susceptible to over-decomposition and modal confusion, so it can extract cleaner high-frequency components. For the subsequent Hilbert transform, it can effectively suppress the impact of noise on instantaneous amplitude acquisition and signal decomposition.

VMD is fundamentally a fully iterative, quasi-orthogonal method for adaptive signal processing. A multi-component signal made up of numerous single components superposed on top of one another can be broken down by VMD into a number of narrowly bandwidth *IMF* components that are tightly focused on their respective core frequencies [30]. The Fourier domain iterative processes of $u_k(t)$ and ω_k are represented by (1)-(2).

$$\hat{u}_k^{n+1}(\omega)=\frac{\hat{f}(\omega)-\sum i\neq k\,\hat{u}(\omega)+\frac{\hat{\lambda}(\omega)}{2}}{1+2\alpha(\omega-\omega_k)^2} \tag{1}$$

$$\omega_k^{n+1}=\frac{\int_0^\infty \omega\left|\hat{u}_k(\omega)\right|^2 d\omega}{\int_0^\infty \left|\hat{u}_k(\omega)\right|^2 d\omega} \tag{2}$$

Where $\hat{u}_k^{n+1}(\omega)$ denotes the Fourier transform of $u_k^{n+1}(t)$ and serves as the Wiener filter for the mode signal; The power spectrum center of gravity that corresponds to the mode function is denoted by ω_k^{n+1}.

The λ expression is obtained after iterations of alternating optimization:

$$\hat{\lambda}^{n+1}(\omega)\leftarrow\hat{\lambda}^{n}(\omega)+\gamma\left(\hat{f}(\omega)-\sum\hat{u}\,k^{n+1}(\omega)\right) \tag{3}$$

Where, γ signifies the tolerance to noise, that satisfies the fidelity criteria necessary for signal decomposition.

The iterative process of VMD to find the optimal solution is as follows:

1) Initialize u_k^1, ω_k^1, and λ_k^1 to zero, select k as a positive integer for decomposition and specify the maximum number of iterations.
2) $\hat{u}_k$ and ω_k are updated by means of (1) and (2).
3) Update $\hat{\lambda}$.
4) The criterion for accuracy convergence is $\varepsilon>0$. If $\sum_k\left\|\hat{u}_k^{n+1}-\hat{u}_k^{n}\right\|_2^2/\left\|\hat{u}_k^{n}\right\|_2^2<\varepsilon$ and $n<N$ are not feel content, the second step is returned; if not the iteration is over and the final $\hat{u}_k$ and ω_k results are produced.

B. Instantaneous Amplitude of VMD-HT

The fault's transient features are more likely to be reflected in the fault current high-frequency component. Therefore, after the fault current is decomposed by VMD, Hilbert transform (HT) is used to calculate the momentary amplitude of high-frequency components as the transient quantity to indicate the fault characteristics in this paper.

After the VMD decomposition of the fault signal, a number of *IMFs* components are obtained, which contains the information of the fault signal in the full frequency domain. Suppose that VMD decomposes the fault signal into n *IMF*s components, which are respectively IMF_1, IMF_2, IMF_3... IMF_n indicates. The Hilbert transformation is performed for each *IMF*. According to the definition of the Hilbert transform [31], the Hilbert signal is as following.

$$\tilde{h}_i(t) = \frac{1}{\pi}\int_{-\infty}^{+\infty}\frac{h_i(\tau)}{t-\tau}d\tau = h_i(t) * \frac{1}{\pi t} \tag{4}$$

Its analytic signal $z_i(t)$ is

$$z_i(t) = h_i(t) + j\tilde{h}_i(t) = a_i(t)e^{j\phi_i(t)} \tag{5}$$

Therefore, it can be further obtained that the $h_i(t)$ amplitude function of the IMF component is as following.

$$a_i(t) = \sqrt{h_i^2(t) + \tilde{h}_i^2(t)} \tag{6}$$

III. Basic Principle of the Proposed Algorithm

A. Construction of Fault Current Traveling Wave Differential Directional Relay

There are lots of power equipment connected with the bus bar of substation, which have stray distributed capacitance to the ground. Numerous high frequency signals will be bypassed by the spread capacitance to ground when the fault high frequency signal travels via the busbar. The high-frequency signal on the incoming bus is significantly greater than that on the outgoing bus [32]. The transient component of 50 kHz–100 kHz experiences significant attenuation or reflection when passing through the bus system. The characteristics of this frequency band can effectively identify fault locations [32]. For this reason, this paper selects the 50 kHz–100 kHz high-frequency band as the object of study. According to these laws, VMD is applied to obtains the high-frequency components from the fault electrical propagation waves at the head of the two lines, and their instantaneous amplitudes are calculated and integrated to obtain IAI_1 and IAI_2, as shown in Fig. 1 Then, the instantaneous amplitude integral difference $IAID = IAI_1 - IAI_2$ is calculated.

In accordance with the law of travelling-wave spreading in the bus system, if the fault occurs in the positive direction of line L_1, $IAI_1 >> IAI_2$, $IAID >> 0$. Therefore, the positive directional fault criterion for line L_1 protection may be established as shown in (7).

$$IAID > +Aset > 0 \tag{7}$$

If the fault occurs in the positive direction of line L_2, there are $IAI_1 << IAI_2$, $IAID << 0$. If the fault is on bus M or line L_3, $IAI_1 \approx IAI_2$, $IAID \approx 0$. Therefore, a positive directional fault for line L_2 protection criterion can be constructed as shown in (8).

$$IAID < -Bset < 0 \tag{8}$$

The *IAID* fault direction relay is defined as a fault direction feature for both line L_1 and line L_2.

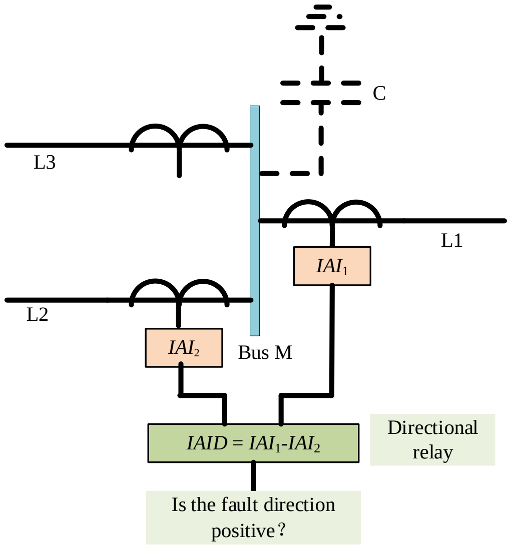

Fig. 1. Instantaneous amplitude difference directional relay

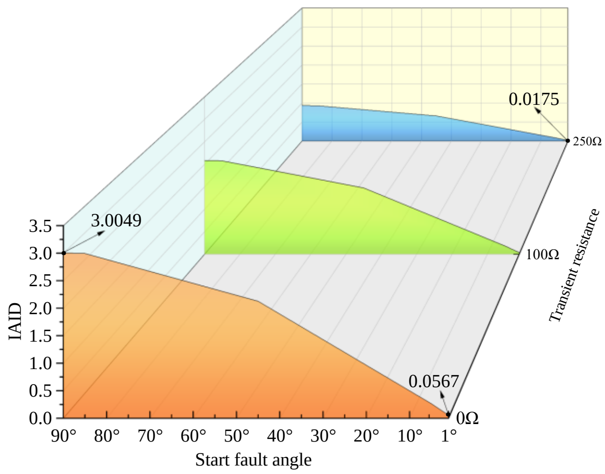

Fig. 2. *IAID* under different fault working conditions

B. Analysis of Fault Condition Attributes' Impact on Protection Reliability

In [19] points out in the paper that the value of fault eigenvalue at an initial fault phase angle of -5° is 0.4% of that at 90°, indicating reduced protection sensitivity. It concludes that the smaller the initial fault phase angle, the lower the protection sensitivity. Reference [19] points out that when start fault phase angle is within the ±18° range around the zero-crossing, it is unable to meet the requirements for protection reliability. The transient resistance and initial fault phase angle also significantly affect the *IAID* amplitude of fault travelling-wave. *IAID* value is displayed in Fig. 2 when internal faults occur under different fault working conditions. As observed from Fig. 2, the *IAID* value decreases as the transition resistance increases and the fault initial angle decreases. For example, the *IAID* value of 0.0567 (θ_f = 1° and R_f = 0 Ω) is 1.9% of 3.0049 (θ_f = 90° and R_f = 0 Ω), and the *IAID* value of 0.0175 (θ_f = 1° and R_f = 250 Ω) is 0.6% of 3.0049 (θ_f = 90° and R_f = 0 Ω). This indicates that the fault condition attributes have a significant impact on the *IAID* values. Traditional method which does not consider the function of fault condition attributes and only sets the action value according to fault characteristics is challenging to guarantee that the protection dependability under all fault conditions can satisfy the requirements. The method of considering fault condition attribute by SVM proposed in this paper will solve this problem.

C. *Protection Algorithm Based on SVM*

In traditional protection, the action value is preset to a constant threshold value in accordance with the different fault characteristic values inside and outside zone. In this method, the fault characteristics are treated as two-dimensional data that changes with time, and the setting value is determined only by considering the fault characteristics. This method has a defect, that is, it does not consider the impact of the start fault phase angle and transient resistance on the fault characteristics. This results in a huge difference in fault features for various fault conditions, and in weak faults (high transient resistance or small start fault angle), the reliability cannot meet the requirements.

In this study, it is discovered that the two main variables influencing the fault characteristic value are the start fault phase angle and the transient resistance, so the fault characteristics are assigned two fault condition attributes, start fault phase angle and transient resistance. The fault characteristics become four-dimensional data with multiple information. When trying to judge a fault, the fault characteristic value can be investigated from the point of view of their fault condition attributes. If different setting values can be given for different fault condition attributes, accuracy of fault detection and protection reliability will be greatly improved.

This kind of requirements, manual method is not competent. Taking forward faults as one category and reverse faults as another category, machine learning can well realize the classification requirements of the above protected areas. Vapnik *et al*. used the statistical learning theory's structural risk minimization concept to create the SVM machine learning algorithm. SVM is a convex quadratic optimization problem that maximizes the generalization ability of machine learning. Compared with neural networks, SVM only needs a smaller training set of samples to achieve better classification results. Therefore, SVM is adopted in this paper to realize fault judgment, and four-dimensional fault characteristic data with two fault condition attributes is used as the input of SVM.

D. *Longitudinal Protection Process*

Conventional differential longitudinal protection relies on high-precision synchronous sampling equipment for strict data synchronization, and conventional transient directional longitudinal protection is susceptible to fault condition attributes, resulting in poor protection reliability. However, in this study, the scheme presented provides their alternative. The *IAID* of the fault current propagating wave on both sides of the bus is used as the fault direction feature to determine the fault direction, and using SVM to integrate the attributes of fault condition into the fault direction feature. In this scheme, In this scheme, rigorous data synchronization at both ends is not required, and reduces the negative effect of the attributes of fault condition on the sensitivity and dependability of transient direction protection, and further improves the stability of the protection by adopting blocking type protection.

Fig. 3 shows the steps involved in the proposed protection algorithm. (1) Collect voltage and current signal from head end of line L_1 and L_2. (2) VMD is applied to extract the high-frequency component of the fault current's traveling wave, and the instantaneous amplitudes of the travelling wave of fault current IAI_1 and IAI_2 are calculated. (3) Calculate the fault direction feature, namely the instantaneous amplitude difference *IAID*, $IAID = IAI_1 - IAI_2$. (4) Calculate the transient resistance R_f and start fault angle θ_f. (5) *IAID*, θ_f and R_f were combined into a composite fault characteristic vector as SVM's inputs. Fault training-sample set is used to train SVM, or the direction is identified using the trained SVM. (6) If it is recognized as a opposite direction fault of the protected line, send a blocking signal to the local unit and the peer unit. (7) If it is recognized that the fault occurs within the positive direction of the protected line, and no blocking signal is received from the protection at the other end of the line, then the fault is determined to be inside the line, and the trip command is sent.

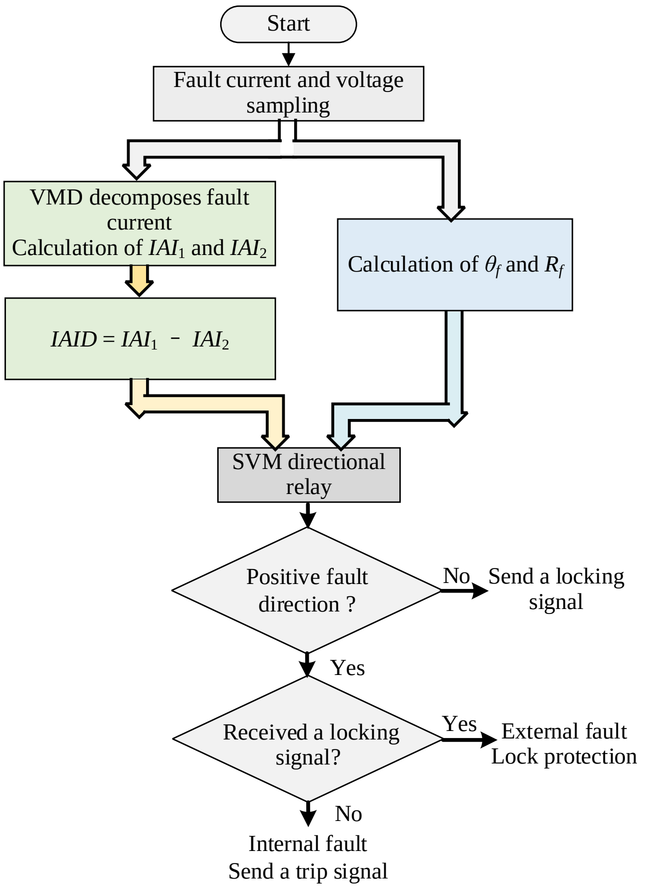

Fig. 3. Protection flow chart

IV. Algorithm Simulation Verification

A. Introduction to Simulation Power Grid Model

The grid connection depicted in Fig. 4 is sourced from the 500kV line of China Southern Power Grid. The AB, BC, and CD segments are 180km, 175km, and 160km respectively. Where S_1=25GV·A, S_2=20GV·A, S_3=15GV·A, S_4=5GV·A. Line parameters X_1=0.2783 Ω/km, C_1=0.01268 μF/km, R_1=0.0271 Ω/km, X_0=0.64938 Ω/km, C_0 = 0.0089 μF/km, R_0 = 0.19478 Ω/km. Distributed capacitance equivalent of each bus to ground is 0.05μF [33]. Line BC is the protected object. The proposed protection is installed at line BC's two ends. The fault direction characteristic of Dir_Relay_1 on the left side is $IAID_{12} = IAI_1\text{-}IAI_2$. When the positive area of line BC (that is, the positive area of Dir_Relay_1.) is faulty, $IAID_{12}$ is greater than 0. The fault direction characteristic of Dir_Relay_2 is $IAID_{34} = IAI_3\text{-}IAI_4$. When the CB positive area of the line (that is, the positive area of Dir_Relay_2.) is faulty, $IAID_{34} > 0$. If and only if $IAID_{12}$ and $IAID_{34}$ are both greater than 0, that is, the fault is in the positive area of Dir_Relay_1 and Dir_Relay_2, it determines the fault is in the protected area, that is, line BC. Otherwise, it determines that the fault is outside zone.

B. Analysis of Typical Fault Examples

In Fig. 4, fault points are set at F_1 (1km away from bus B) in section AB, F_2 (1km away from bus B) and F_3 (1km away from bus C) in section BC, F_4 (1km away from bus C) in section CD, F_5 of bus B and F_6 of bus C. At each fault point, various fault conditions are simulated. During the simulation, start fault angle θ_f varies at 0°-360°, and transient resistance R_f varies at 1Ω-300Ω. The sampling frequency of fault current and voltage signal is 400 kHz. The data window length was set to 200 samples, i.e. 0.5ms. Due to the limitation of space, the following only takes the A-contact ground fault as an example for analysis, and only some typical data are listed.

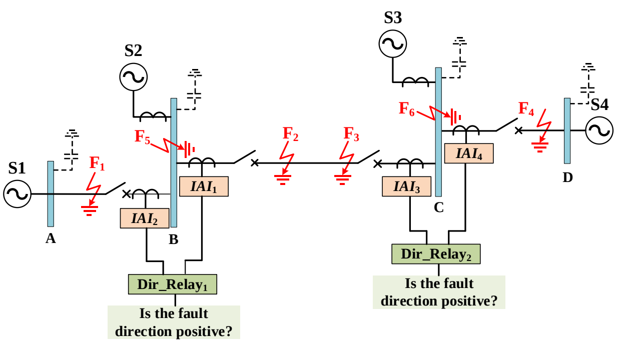

Fig. 4. Simulation system diagram

1) Line AB Fault

If an A-phase ground fault is at F_1 point on line AB where is 1km away from bus B, θ_f is 85° and R_f is 5Ω, $IAID_{12}$ and $IAID_{34}$ are shown in Fig. 5. If $IAID_{12}$ is much smaller than 0, it shows that the fault is located in line BC's opposite direction. If $IAID_{34} > 0$, it shows that the fault is located in line CB's positive direction. Therefore, the fault is determined to be occurring outside region.

When the fault is at F_1 point, the change of $IAID_{12}$ and $IAID_{34}$ with the change of the transient resistance and start fault angle is shown in Table I. If the fault is at F_1, $IAID_{12}$ is less than 0 and $IAID_{34} > 0$, it shows that the fault is in the opposite direction of Dir_Relay_1 and in the positive direction of Dir_Relay_2. It shows that the fault is at outside area. The data in Table II show that when θ_f changes from 90° to 0°, $|IAID_{12}|$ and $|IAID_{34}|$ become significantly smaller. When R_f changes from 0 Ω to 250 Ω, $|IAID_{12}|$ and $|IAID_{34}|$ decrease obviously.

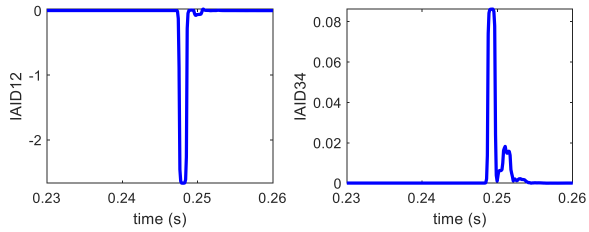

Fig. 5. $IAID$ of F_1 fault with θ_f=85°, R_f =5Ω

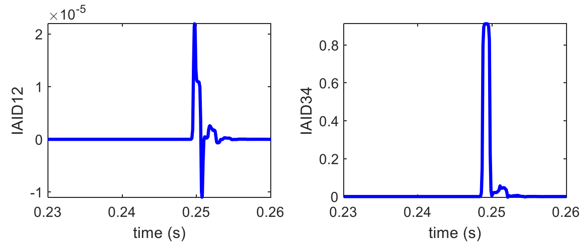

Fig. 6. $IAID$ of F_5 fault with θ_f=85°, R_f =5Ω

TABLE I
$IAID$ OF F_1 FAULT WITH DIFFERENT θ_f AND R_f

	θ_f (°)	R_f (Ω)			
		0	50	100	250
$IAID_{12}$	1	-0.0527	-0.0428	-0.0362	-0.0247
	3	-0.1473	-0.1204	-0.1019	-0.0697
	5	-0.2438	-0.1995	-0.1689	-0.1155
	45	-1.9399	-1.5898	-1.3460	-0.9208
	85	-2.7302	-2.2378	-1.8946	-1.2962
	90	-2.7404	-2.2461	-1.9017	-1.3010
$IAID_{34}$	1	0.0017	0.0014	0.0012	0.0008
	3	0.0047	0.0039	0.0033	0.0023
	5	0.0079	0.0065	0.0055	0.0038
	45	0.0626	0.0515	0.0438	0.0302
	85	0.0881	0.0726	0.0617	0.0425
	90	0.0884	0.0728	0.0619	0.0426

TABLE II
$IAID$ OF F_5 FAULT WITH DIFFERENT θ_f AND R_f

	θ_f (°)	R_f (Ω)			
		0	50	100	250
$IAID_{12}$	1	6.99E-06	3.04E-05	3.48E-05	4.04E-05
	3	5.88E-06	2.75E-05	3.11E-05	3.55E-05
	5	5.04E-06	2.59E-05	2.93E-05	3.37E-05
	45	7.56E-06	4.10E-06	9.56E-06	2.10E-05
	85	1.16E-05	9.26E-06	1.15E-05	1.71E-05
	90	1.18E-05	1.04E-05	1.27E-05	1.79E-05
$IAID_{34}$	1	0.0185	0.0096	0.0059	0.0027
	3	0.0516	0.0272	0.0166	0.0076
	5	0.0854	0.0451	0.0276	0.0125
	45	0.6791	0.3596	0.2203	0.1000
	85	0.9557	0.5062	0.3101	0.1408
	90	0.9593	0.5081	0.3113	0.1413

2) Fault on Bus B

When A-phase ground fault occurs at F_5 point on bus B, θ_f is 85° and R_f is 5Ω, $IAID_{12}$ and $IAID_{34}$ are shown in Fig. 6. The absolute value of $IAID_{12}$ is very small, very close to 0, and fluctuates around 0. Bus B is in the negative-direction area of directional relay Dir_Relay$_1$. While $IAID_{34}$ > 0, the fault is in the positive area of Dir_Relay$_2$. In this case, the fault is at outside zone.

When the fault occurs at F_5, the changes of $IAID_{12}$ and $IAID_{34}$ with changes in θ_f and R_f are shown in Table II. $IAID_{12}$ are all close to 0 with very small absolute values. At this time, the fault happens in the opposite direction of line BC. While $IAID_{34}$ > 0, the fault is in the positive area of Dir_Relay$_2$. In this case, the fault is outside the zone.

3) Fault in Line BC

If a A-phase ground fault is at point F_2 of line BC that is 1km away from bus B, θ_f is 85° and R_f is 5Ω, $IAID_{12}$ and $IAID_{34}$ are shown in Fig. 7. Since $IAID_{12}$ > 0, it shows that the fault occurs in the positive direction of line BC. Since $IAID_{34}$ > 0, it shows that the fault occurs in the positive direction of CB. Therefore, the fault occurs within the zone.

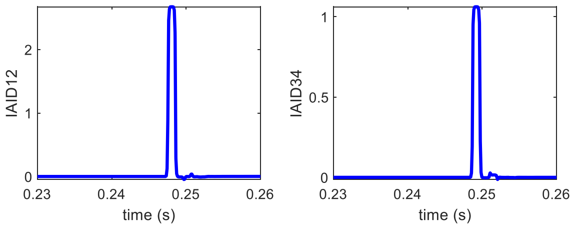

Fig. 7. *IAID* of F_2 fault with θ_f =85°, R_f =5Ω

When the fault is at F_2 point, the change of $IAID_{12}$ and $IAID_{34}$ with the change of the transient resistance and start fault angle is shown in Table III. While a fault is located at F_2, $IAID_{12}$ > 0, and $IAID_{34}$ > 0, it shows that the fault is in the positive area of Dir_Relay$_1$ and Dir_Relay$_2$. It shows that the fault occurred within the protected area. The data in Table III show that when θ_f changes from 90° to 0°, $|IAID_{12}|$ and $|IAID_{34}|$ decrease significantly. When R_f changes from 0 Ω to 250 Ω, $|IAID_{12}|$ and $|IAID_{34}|$ decrease obviously.

TABLE III
IAID OF F_2 FAULT WITH DIFFERENT FAULT CONDITION ATTRIBUTES

	θ_f (°)	R_f (Ω)			
		0	50	100	250
$IAID_{12}$	1	0.0517	0.0420	0.0356	0.0243
	3	0.1463	0.1196	0.1012	0.0693
	5	0.2429	0.1988	0.1683	0.1151
	45	1.9396	1.5896	1.3459	0.9208
	85	2.7309	2.2383	1.8951	1.2965
	90	2.7411	2.2467	1.9022	1.3014
$IAID_{34}$	1	0.0203	0.0167	0.0142	0.0098
	3	0.0579	0.0476	0.0404	0.0278
	5	0.0963	0.0792	0.0672	0.0462
	45	0.7706	0.6337	0.5378	0.3696
	85	1.0850	0.8923	0.7573	0.5205
	90	1.0891	0.8956	0.7601	0.5224

When an A-phase grounding fault is at F_3 point 1km away from bus C on line BC, the changes of $IAID_{12}$ and $IAID_{34}$ with changes in θ_f and R_f are shown in Table IV. If $IAID_{12}$ > 0, and $IAID_{34}$ > 0, the fault is in the positive area of Dir_Relay$_1$ and Dir_Relay$_2$. It shows that the fault occurred within the protected area.

TABLE IV
IAID OF F_3 FAULT WITH DIFFERENT FAULT CONDITION ATTRIBUTES

	θ_f (°)	R_f (Ω)			
		0	50	100	250
$IAID_{12}$	1	0.0219	0.0179	0.0152	0.0104
	3	0.0615	0.0505	0.0429	0.0295
	5	0.1020	0.0838	0.0711	0.0489
	45	0.8133	0.6687	0.5676	0.3901
	85	1.1448	0.9414	0.7990	0.5492
	90	1.1491	0.9449	0.8020	0.5512
$IAID_{34}$	1	0.0545	0.0447	0.0378	0.0259
	3	0.1544	0.1265	0.1071	0.0733
	5	0.2563	0.2101	0.1779	0.1217
	45	2.0465	1.6774	1.4202	0.9716
	85	2.8813	2.3616	1.9995	1.3679
	90	2.8921	2.3705	2.0070	1.3731

4) Fault at Bus C

When A-phase ground fault occurs at F_6 on bus C, θ_f is 85° and R_f is 5Ω, $IAID_{12}$ and $IAID_{34}$ are shown in Fig. 8. When $IAID_{12}$ > 0, the fault is in the positive area of Dir_Relay$_1$. The absolute value of $IAID_{34}$ is very small, very close to 0, and fluctuates around 0. Bus C is located in the reverse direction area of directional relay Dir_Relay$_2$. In this case, the fault is at outside zone.

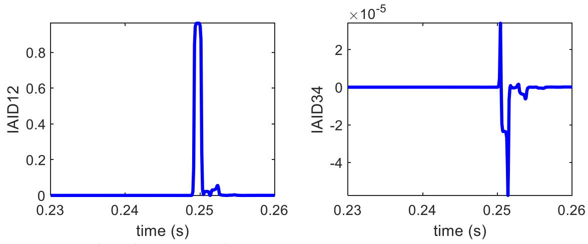

Fig. 8. *IAID* of F_6 fault with θ_f =85°, R_f =5Ω

TABLE V
IAID OF F_6 FAULT WITH DIFFERENT FAULT CONDITION ATTRIBUTES

	θ_f (°)	R_f (Ω)			
		0	50	100	250
$IAID_{12}$	1	0.0190	0.0099	0.0060	0.0028
	3	0.0539	0.0284	0.0174	0.0079
	5	0.0896	0.0473	0.0290	0.0132
	45	0.7166	0.3794	0.2324	0.1055
	85	1.0090	0.5343	0.3274	0.1486
	90	1.0128	0.5364	0.3286	0.1492
$IAID_{34}$	1	1.94E-04	6.92E-05	4.89E-05	3.11E-05
	3	1.75E-04	6.57E-05	4.56E-05	2.77E-05
	5	1.70E-04	6.50E-05	4.55E-05	2.77E-05
	45	9.86E-05	3.90E-05	2.95E-05	2.22E-05
	85	2.61E-05	7.59E-06	3.80E-06	8.83E-07
	90	1.69E-05	3.48E-06	4.44E-07	-1.75E-06

When the fault occurs at F_6, the changes of $IAID_{12}$ and $IAID_{34}$ with changes in θ_f and R_f are shown in Table V. If

$IAID_{12}$ > 0, the fault is in the positive area of Dir_Relay_1. $IAID_{34}$ are all close to 0 and has either positive or negative values. In this case, the fault is at outside zone.

5) Fault in Line CD

When a A-phase ground fault is at F_4 point of line CD where is 1km away from bus C, θ_f is 85° and R_f is 5Ω, $IAID_{12}$ and $IAID_{34}$ are shown in Fig. 9. Since $IAID_{12}$ > 0, the fault is at line-BC's positive direction zone. Since $IAID_{34}$ is much smaller than 0, it shows that the fault lies in line CB's reverse direction. Therefore, the failure occurs outside the zone.

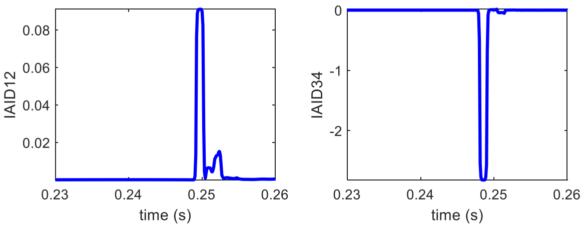

Fig. 9. *IAID* of F_4 fault with θ_f=85°, R_f =5Ω

When the fault happens at F_4 point, the changes of $IAID_{12}$ and $IAID_{34}$ with changes in θ_f and R_f are shown in Table VI. When the fault is at F_4, $IAID_{12}$ > 0, indicating that the fault lies in the forward direction of Dir_Relay_1. For $IAID_{34}$ is less than 0, the fault happens in the negative-direction zone of Dir_Relay_2. Therefore, it shows that the failure occurred outside the protected area.

TABLE VI
IAID OF F_4 FAULT WITH DIFFERENT FAULT CONDITION ATTRIBUTES

	θ_f (°)	R_f (Ω)			
		0	50	100	250
$IAID_{12}$	1	0.0022	0.0016	0.0013	0.0009
	3	0.0053	0.0042	0.0036	0.0025
	5	0.0086	0.0069	0.0059	0.0041
	45	0.0662	0.0545	0.0463	0.0319
	85	0.0930	0.0766	0.0651	0.0448
	90	0.0933	0.0768	0.0653	0.0450
$IAID_{34}$	1	-0.0551	-0.0452	-0.0383	-0.0262
	3	-0.1550	-0.1271	-0.1076	-0.0736
	5	-0.2570	-0.2107	-0.1784	-0.1220
	45	-2.0478	-1.6785	-1.4211	-0.9722
	85	-2.8824	-2.3626	-2.0003	-1.3685
	90	-2.8932	-2.3714	-2.0078	-1.3736

C. Fault Determination Based SVM and Discussion

The application of SVM to judge the fault direction is to classify the fault direction with SVM. First, a forward region fault category is defined for directional relays Dir_Relay_1 and Dir_Relay_2, denoted by 1. Faults in other locations belong to the reverse zone faults, which are defined as another category and are represented by -1. According to the analysis in Section 4.2, the forward region of Dir_Relay_1 includes the positions F_2, F_3, F_4, and F_6 in Fig. 4. The points F_1 and F_5 belong to the reverse region of Dir_Relay_1. The forward region of Dir_Relay_2 includes the F_3, F_2, F_5, and F_1 positions shown in Fig. 4. The F_6 and F_4 points belong to the inverse region of Dir_Relay_2.

SVM needs to be trained. The data in Table I-VI are classified into training sample set and testing sample combination. The training sample set includes fault data with fault condition attributes of 1°, 5°, 45°, 85° and 90°. The test sample set composed of fault data with fault condition attribute of 3°. The four-dimensional composite fault feature vector composed of *IAID*, θ_f, and R_f is used as the input vector of SVM of relay Dir_Relay, and the output of SVM is fault direction class 1 or -1. After the training of SVM fault direction classification is completed with the training sample set, the trained SVM is used to test with the test sample set to determine the fault direction.

The proposed method shows strong fault identification even under weak fault conditions. Taking an internal fault at F_2 with extreme parameters (θ_f =1°, R_f =250 Ω) as a representative case study, the measured *IAID* merely reaches 0.0243. In this case, a conventional protection scheme that relies solely on *IAID* judgement is likely to fail to trip. However, our SVM-based direction preservation solves this challenge through a nonlinear feature space transformation. By using θ_f, R_f, and *IAID* as multidimensional input vectors, the original measurement point (*IAID*=0.0243, θ_f =1°, R_f =250 Ω) can be mapped to the equivalent high sensitivity domain (*IAID*=2.7411, θ_f =90°, R_f =0 Ω). By compensating for the combined effect of a small θ_f and a large R_f, reliable fault direction discrimination is achieved, which significantly improves protection sensitivity and reliability. The experimental results displayed that the correct rate of fault direction judgment was 100%.

It is worth noting that though the test sample set is raw data which is not used to train SVM, the fault direction judgment is still correct, indicating that the SVM method has good generalization ability. These results show that in the process of fault judgment in practical engineering, SVM only needs to be trained with the typical fault sample set, and the correct judgment can be made for those faults that are not in the training sample set. It is an effective method to judge the fault of relay protection.

For reasons of space limitation, the above only lists the research of single-phase grounding fault. For other types of fault judgment research, the above method is equally effective.

V. Conclusion

According to the law of transient signal attenuation through the bus and the influence of two attributes of fault condition on the *IAID* of travelling wave current, a novel method of pilot protection algorithm relying on the *IAID* of travelling wave current and SVM is presented. In this algorithm, the fault feature vector, composed of the fault direction feature and fault condition attribute, is used as the input for SVM. The fault condition attribute is integrated into the fault direction feature. Based on this, SVM identifies the fault direction by dynamically adjusting the action threshold based on the variation in fault condition attributes. EMTP-RV is applied to validate the correctness of the presented algorithm through a large number of simulations. The results show that the designed protection scheme has the following advantages:

1) The method in this paper does not need to extract the travelling wave head, and compared with the traditional

directional longitudinal protection only need to extract the current travelling wave to judge the fault, which improves the stability of the system.

2) The fault condition attribute is fused into the fault feature vector to overcome its adverse influence on protection. It solved protection's insufficient sensitivity when the fault is within 18° of the traditional direction protection crossing point, and improved the reliability by 10%.
3) An fault current traveling wave differential direction relay can simultaneously identify the fault direction of two related lines. fault traveling wave differential.
4) Lots of simulation tests verified that the presented algorithm can precisely determine internal and external fault for all fault conditions, and it is a potential transient direction longitudinal protection method.

REFERENCES

[1] Hongchun Shu, Kaiqing Tian, Yutao Tang, Yue Dai, "Novel protection scheme for EHV transmission line based on traveling wave energy," *Electric Power Systems Research*, vol. 230, pp110247, 2024.

[2] Wu H, Dong XX, Ye RK, "A new algorithm for busbar protection based on the comparison of initial traveling wave power," *IEEJ Transactions on Electrical & Electronic Engineering*, vol. 14, no. 4, pp520–533, 2019.

[3] Liu Y, Huang Z, Xie X, *et al.*, "Redox flow battery: Flow field design based on bionic mechanism with different obstructions," *Chemical Engineering Journal*, vol. 498, pp155663, 2024.

[4] P. Lertwanitrot, P. Kettranan, P. Itthisathienkul, A. Ngaopitakkul, "Characteristics and Behaviour of Transient Current during Lightning Strikes on Transmission Tower," *Lecture Notes in Engineering and Computer Science*, vol.2216, no.1, pp708-713, 2015.

[5] F. Namdari and M. Salehi, "High-Speed Protection Scheme Based on Initial Current Traveling Wave for Transmission Lines Employing Mathematical Morphology," *IEEE Transactions on Power Delivery*, vol. 32, no. 1, pp246-253, 2017.

[6] Bowen Zheng , Lu Chu and Zengping Wang, "Transient Protection Principle Based on Current Ratio of Two Terminals in Frequency Domain," *Electronics*, vol. 11, no. 9, pp1463, 2022.

[7] Guo ZW, Deng YC, Huang JM, Zhang T, Huang ZB, "A novel S-Transform-based pilot protection algorithm for transmission lines," *Electric Power Systems Research*, vol. 241, pp111321, 2025.

[8] Guo ZW, Yang SJ, *et al.*, "Non-communication protection scheme for power transmission system based on transient currents HHT and SVM," *IET Generation, Transmission & Distribution*, vol. 12, no. 12, pp2816-2824, 2018.

[9] Jin N, Rong Z, Lin X, *et al.*, "A novel principle of line pilot protection based on the recognition of phase space trajectory of fault component instantaneous power," *Proceedings of the Chinese Society for Electrical Engineering*, vol. 39, no. 9, pp2702–2712, 2019.

[10] Wang Q, Xu XD, "Applied criterion for line protection based on traveling-wave differential principle," *Automation of Electric Power Systems*, vol. 36, no. 1, pp86–89, 2012.

[11] Yutao Tang, Hongchun Shu, Yue Dai, Yiming Han, "Enhanced pilot protection scheme for half-wavelength transmission line based on the conservation of traveling wave energy," *International Journal of Electrical Power & Energy Systems*, vol. 161, pp110184, 2024.

[12] Zhengyou He, Shibin Gao, et al., "Study of a new method for power system transients classification based on wavelet entropy and neural network," *International Journal of Electrical Power & Energy Systems*, vol. 33, no. 3, pp402-410, 2011.

[13] Xiaoyan Xu, "Research on a Small Target Object Detection Algorithm for Electric Transmission Lines Based on Convolutional Neural Network," *IAENG International Journal of Computer Science*, vol. 50, no. 2, pp375-380, 2023.

[14] Xingchen Song, Tongxi Wang, Ziming Xu, and Zhan Shi, "Multistep Forecasting Method of Short-term Power Load Based on VMD-Prophet-Seq2seq," *IAENG International Journal of Computer Science*, vol. 49, no. 3, pp720-727, 2022.

[15] Shuhao Liu, Kunlun Han, Hongzheng Li, Tengyue Zhang, Fengyuan Chen, "A Two-Terminal Directional Protection Method for HVDC Transmission Lines of Current Fault Component Based on Improved VMD-Hilbert Transform," *Energies*, vol. 16, no. 19, pp6987, 2023.

[16] Yuqi Wu, Zhengtian Li, Xiangning Lin, *et al.*, "A Novel Single-Ended Transient-Based Boundary Protection Based on the Instantaneous Energy of Traveling Waves," *IEEE Transactions on Power Delivery*, vol. 39, no. 3, pp1-5, 2024.

[17] Wei Chen, O. P. Malik, Xianggen Yin, Deshu Chen, Zhe Zhang, "Study of wavelet-based ultra high speed directional transmission line protection," *IEEE Transactions on Power Delivery*, vol. 18, no. 4, pp1134-1139, 2003.

[18] X. Dong, Y. Ge, J. He. "Surge impedance relay," *IEEE Transactions on Power Delivery*, vol. 20, no. 2, pp1247-1256, 2005.

[19] J. Duan, B. Zhang. "Research on ultra-high-speed directional relay of EHV/UHV transmission lines using wavelet transform," *WSEAS Transactions on Circuits and Systems*, vol. 3, no. 4, pp896-901, 2004.

[20] Aoyu Lei, Xinzhou Dong, Vladimir Terzija, "An Ultra-High-Speed Directional Relay Based on Correlation of Incremental Quantities," *IEEE Transactions on Power Delivery*, vol. 33, no. 6, pp2726-2735, 2018.

[21] Xinzhou Dong, Shiyong Wang, Shenxing Shi, "Polarization current travelling wave direction relay," *Power System Automation*, vol. 35, no. 21, pp78-83, 2011.

[22] Zhenwei Guo, Jiangang Yao, Shengjie Yang, *et al.*, "A new method for non-unit protection of power transmission lines based on fault resistance and fault angle reduction," *International Journal of Electrical Power and Energy Systems*, vol. 55, pp760-769, 2014.

[23] P. Jafarian, M. Sanaye-Pasand, "High-Frequency Transients-Based Protection of Multiterminal Transmission Lines Using the SVM Technique," *IEEE Transactions on Power Delivery*, vol. 28, no. 1, pp188-196, 2013.

[24] Guo ZW, Yao JG, Jiang YC, *et al.*, "A novel distributed unit transient protection algorithm using support vector machines," *Electric Power Systems Research*, vol. 123, pp13-20, 2015.

[25] Pengfei Tian, You Yu, Ming Dong, *et al.*, "A CNN-SVM-based fault identification method for high-voltage transmission lines," *Power System Protection and Control*, vol. 50, no. 13, pp119-125, 2022.

[26] K. Seethalekshmi, S. N. Singh, S. C. Srivastava, "A Classification Approach Using Support Vector Machines to Prevent Distance Relay Maloperation Under Power Swing and Voltage Instability," *IEEE Transactions on Power Delivery*, vol. 27, no. 3, pp1124-1133, 2012.

[27] Ouyang Xinyu, Zhao Nannan, Gao Chuang, Wang Lidong, "An Efficient Twin Projection Support Vector Machine for Regression," *Engineering Letters*, vol. 27, no. 1, pp103-107, 2019.

[28] Qinghe Zheng, Xinyu Tian, Mingqiang Yang, Huake Su, "The Email Author Identification System Based on Support Vector Machine (SVM) and Analytic Hierarchy Process (AHP)," *IAENG International Journal of Computer Science*, vol. 46, no. 2, pp178-191, 2019.

[29] Xiaowei Wang, Fan Zhang, Jie Gao, *et al*., "Fault location based on variable mode decomposition and kurtosis calibration in distribution networks," *Electrical Power and Energy Systems*, vol. 154, pp109463, 2023.

[30] Yanchun Xu, Caicai Zhao, Shasha Xie, Mi Lu, "Novel Fault Location for High Permeability Active Distribution Networks Based on Improved VMD and S-transform," *IEEE Access*, vol. 9, pp17662-17671, 2021.

[31] Espinosa Antonio Garcia, Rosero Javier A., Cusidó Jordi, Romeral Luis, Ortega Juan Antonio, "Fault Detection by Means of Hilbert–Huang Transform of the Stator Current in a PMSM With Demagnetization," *IEEE Transactions on Energy Conversion*, vol. 25, no. 2, pp312-318, 2010.

[32] Bo ZQ. "A new non-communication protection technique for transmission lines," *IEEE Transactions on Power Delivery*, vol. 13, pp1073-1078, 1998.

[33] D. Povh, H. Schmitt, O. Volcker, *et al*., "Modeling and Analysis Guidelines for Very Fast Transients," *IEEE Power Engineering Review*, vol. 16, no. 10, pp71, 1996.